Heat Convection from a Sphere Placed in a Fluctuating Free Stream

R. S. Alassar
Dept. of Mathematical Sciences, King Fahd University of Petroleum & Minerals, Dhahran, Saudi Arabia

H. M. Badr
Dept. of Mechanical Engineering, King Fahd University of Petroleum & Minerals, Dhahran, Saudi Arabia

DOI 10.1002/aic.11199
Published online May 16, 2007 in Wiley InterScience (www.interscience.wiley.com).

The effect of sinusoidal fluctuations superimposed on the average free-stream velocity on mixed convection from a spherical particle is investigated. The parameters considered are the Reynolds number Re, Grashof number Gr*, and the relative amplitude of fluctuations. The results indicate that due to the adverse pressure gradients created by the deceleration of the free-stream, separation may occur at a Reynolds number well below that at which it occurs in uniform flow. The rising buoyancy currents, however, weaken and possibly destroy the formation of vortices at the rear stagnation point. The average Nusselt number is found to increase with the increase of the amplitude of the free stream fluctuations and with the increase of* Gr/Re^2*, as along as the flow does not reverse its direction. The time and space averaged Nusselt number increases with* Gr/Re^2*, with the effect of the amplitude of the free-stream fluctuations becoming less pronounced at higher values of* Gr/Re^2*.* © 2007 American Institute of Chemical Engineers *AIChE J,* 53: 1670–1677, 2007
Keywords: heat convection, sphere, fluctuating flow, buoyancy

Introduction

The problem of heat transfer from a sphere has been the subject of many investigations due to the related engineering applications. Several experimental and theoretical studies can be found which deal with either free, forced, or mixed (combined free and forced) convection from a sphere placed in a free-stream. The classical studies which investigate only free convection are those by Potter and Riley,[1] Geoola and Cornish[2] and,[3] Riley,[4] Brown and Simpson,[5] Singh and Hasan,[6] and Dudek et al.[7] Representative work on forced convection from a sphere placed in a steady uniform stream are the studies by Dennis and Walker[8] for Reynolds number up to 200, Whitaker,[9] the highly accurate and detailed results by Dennis et al.[10] but for Reynolds number up to 20, and Sayegh and Gauvin.[11] The mixed convection problem was studied at small Reynolds and Grashof numbers by Hieber and Gebhart.[12] The problem was also solved using the boundary layer approach by Acrivos.[13] Wong and Chen[14] used finite differences to solve the full steady Navier-Stokes and energy equations. Nguyen et al.[15] extended the work of Wong and Chen[14] and solved the transient problem with internal thermal resistance.

The structure of the flow field under an oscillating free stream is important in understanding the heat convection process. Several studies on oscillating flow which do not consider any heat-transfer processes are available. The interested reader is directed to the studies by Basset,[16] Odar and Hamilton,[17] Mei,[18] Lawrence and Mei,[19] Sano,[20] Lovalenti and Brady,[21] Mei et al.[22] Riley,[23] and Chang and Maxey.[24] A review of the literature can be found in Alassar and Badr[25] who extended the work of Chang and Maxey[24] to Reynolds number of 200, and included a detailed analysis of the separation angle and the wake length.

The studies on heat or mass transfer from a sphere in an oscillating free-stream are, on the other hand, few. The two

Correspondence concerning this article should be addressed to R. S. Alassar at alassar@kfupm.edu.sa.

articles by Drummond and Lyman,[26] and by Ha and Yavuzkurt[27] deal with forced convection only. Drummond and Lyman[26] studied mass transfer from a sphere in an oscillating flow using a pseudo-spectral method, and concluded that the mass-transfer rate decreases with the decrease of the Strouhal number until the value of 2.0, below which the rate is virtually independent of the Strouhal number. The conclusion of Drummond and Lyman[26] contradicted other experimental and theoretical studies among which are the studies on heat transfer from a sphere in an oscillating and fluctuating free-stream by Ha and Yavuzkurt.[27,28] These studies, however, deal with forced convection, and the effect of gravity is never considered. Alassar et al.[29] considered mixed convection (both forced and free) from a sphere in a purely oscillating vertical free-stream. As the free-stream considered was purely oscillating (about a zero mean), the parameters considered were Reynolds number, Grashof number, and Strouhal number. The study revealed that the phase lag between the free-stream oscillations and the momentum, and thermal-boundary layers decreases with the decrease of Strouhal number. The overall rate of heat transfer exhibits a minimum at a certain critical value of Strouhal number at which the double boundary layer structure disappears. Due to mixed convection, the overall Nusselt number was found to fluctuate at one half of the frequency detected in the case of forced convection with a considerable deviation in the local Nusselt number distribution. Contrary to the case of steady uniform flow, a small increase of Gr/Re^2 may cause appreciable increase in the overall heat transfer in oscillating flow.

The study of Alassar et al.[29] considers a purely oscillating free-stream; that is, the oscillations are about a zero-mean velocity. This article investigates the effect of the free-stream fluctuations about a nonzero mean on the heat transfer from a sphere with buoyancy forces taken into consideration. This study is motivated by the fact that local oscillations imposed on a nonzero-mean flow are frequently encountered in industries. For example, in the initial stage of the combustion of pulverized coal or coal-water slurry droplets, there exists a steady slip velocity U_o, before coal particles or particle agglomerate become entrained in the main gas flow. In order to consider the effect of this steady slip velocity, an oscillating flow induced by the longitudinal high-intensity acoustic field is superimposed on the mean-steady flow.[28] The importance of this research, therefore, in addition to being interesting from an academic point of view, is that it serves several applications. It makes it possible to understand the heat and mass transfer to and from fuel particles and droplets. The results are of use in industries involving pulverized coal particles, coal-water slurry fuel systems, and paint powder technology. Other applications of this research include Brownian motion, suspension rheometry, the passage of sound waves through particulate systems, and extraction of oil from sand particles in depleted oil fields.

Formulation and Method of Solution

We consider a solid spherical particle of dia. 2a suspended in an unbounded fluctuating incompressible stream. The particle is at a constant temperature T_s, which is hotter than the free-stream whose temperature is maintained at T_∞ as sketched in Figure 1.

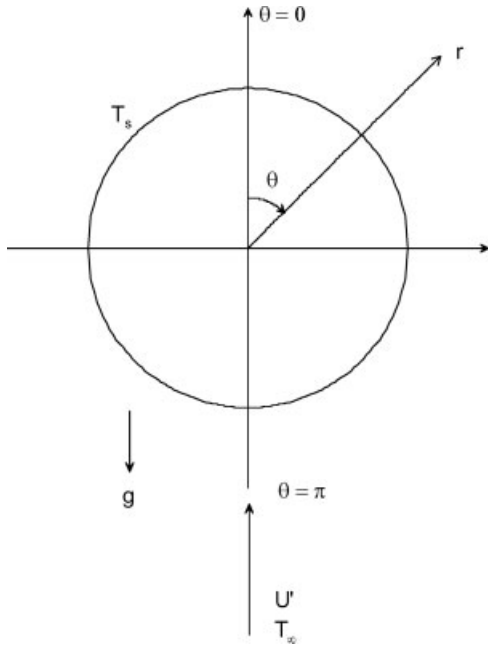

Figure 1. Physical system.

The equations governing the heat-transfer process, in spherical coordinates, can be written in terms of the dimensionless vorticity ζ, the dimensionless stream function ψ, and the dimensionless temperature φ as

$$e^{3\xi}\sin\theta\zeta+\frac{\partial^2\psi}{\partial\xi^2}+\frac{\partial^2\psi}{\partial\theta^2}-\frac{\partial\psi}{\partial\xi}-\cot\theta\frac{\partial\psi}{\partial\theta}=0 \tag{1}$$

$$e^{2\xi}\frac{\partial\zeta}{\partial t}+\frac{e^{-\xi}}{\sin\theta}\left[\frac{\partial\psi}{\partial\theta}\left(\frac{\partial\zeta}{\partial\xi}-\zeta\right)-\frac{\partial\psi}{\partial\xi}\left(\frac{\partial\zeta}{\partial\theta}-\cot\theta\zeta\right)\right]=\frac{2}{\mathrm{Re}}\left[\frac{\partial^2\zeta}{\partial\xi^2}+\frac{\partial^2\zeta}{\partial\theta^2}+\frac{\partial\zeta}{\partial\xi}+\cot\theta\frac{\partial\zeta}{\partial\theta}-\frac{\zeta}{\sin^2\theta}\right]-e^{\xi}\frac{\mathrm{Gr}}{2\mathrm{Re}^2}\left[\sin\theta\frac{\partial\varphi}{\partial\xi}+\cos\theta\frac{\partial\varphi}{\partial\theta}\right] \tag{2}$$

$$e^{2\xi}\frac{\partial\varphi}{\partial t}+\frac{e^{-\xi}}{\sin\theta}\left[\frac{\partial\psi}{\partial\theta}\frac{\partial\varphi}{\partial\xi}-\frac{\partial\psi}{\partial\xi}\frac{\partial\varphi}{\partial\theta}\right]=\frac{2}{Pe}\left[\frac{\partial^2\varphi}{\partial\xi^2}+\frac{\partial^2\varphi}{\partial\theta^2}+\frac{\partial\varphi}{\partial\xi}+\cot\theta\frac{\partial\varphi}{\partial\theta}\right] \tag{3}$$

where t is time, $\mathrm{Re}=2aU_o/\nu$ is the Reynolds number, U_o is the mean free-stream velocity, $Gr=g\sigma(T_s-T_\infty)(2a)^3/\nu^2$ is the Grashof number, T is the temperature, $Pe=Re\,Pr$ is the Peclet number, $Pr=\nu/\alpha$ is the Prandtl number, α is the thermal diffusivity, ν is the coefficient of kinematic viscosity, g is the gravitational acceleration, σ is the coefficient of volumetric thermal expansion, and $\xi=\ln(r/a)$ with r being the dimensional radial distance. The variables ψ, ζ, φ, and t^* (the star is dropped in Eqs. 1–3) in the governing equations

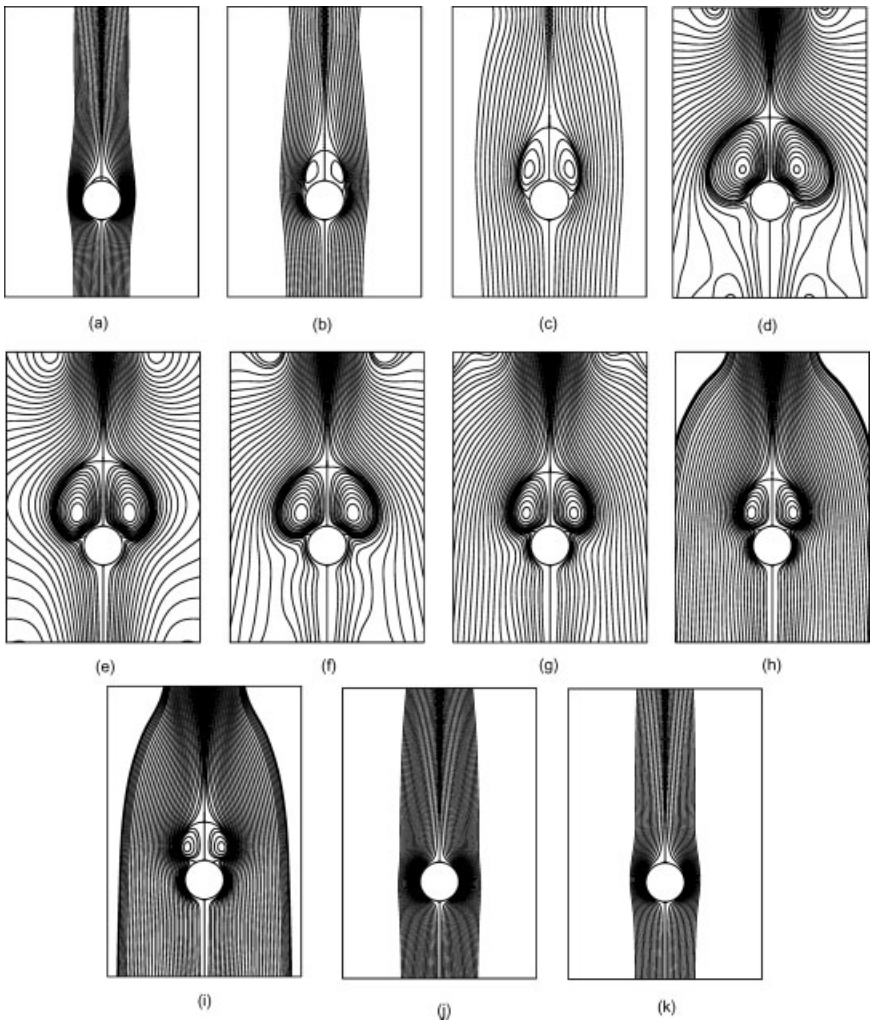

Figure 2. Streamlines for the case Re = 50, *Gr* = 2,500, and $\beta = 1$.

τ = (a) 0.0000, (b) 0.2500, (c) 0.3750, (d) 0.4900, (e) 0.5000, (f) 0.5200, (g) 0.5400, (h) 0.5600, (i) 0.5800, (j) 0.7500, and (k) 0.8750.

are defined in terms of the usual dimensional quantities ψ', ζ', T, and t as $\psi = \psi'/U_o a^2$, $\zeta = \zeta' a/U_o$, $\varphi = (T - T_\infty)/(T_s - T_\infty)$, and $t^* = U_o\, t/a$.

The fluctuations of the free-stream velocity are given in the form $U = U'/U_o = 1 + \beta \cos(St)$ where U' is the dimensional free-stream velocity, β is the amplitude of fluctuations relative to the mean free-stream velocity, and $S = a\omega/U_o$ is the Strouhal number with ω being the frequency of oscillations.

The method of solution is similar to that used by Alassar et al.[29] and need not be written in details. The method uses a Legendre series truncation method to solve the governing equations subject to the boundary conditions. The boundary conditions to be satisfied are the no slip and impermeability conditions on the surface of the sphere, and the free-stream conditions away from it in addition to the thermal conditions. The accuracy of the method of solution was verified by Alassar et al.[29] through comparisons with the forced and mixed convection cases available in the literature, such as Wong et al.[14] Sayegh and Gauvin,[11] Dennis and Walker,[8] and others. The comparisons were satisfactory.

Results and Discussions

The effects of buoyancy forces and the free-stream fluctuations on the flow and thermal fields are investigated for Reynolds numbers Re = 10, 20, 50, 100, and 200, and for Gr/Re^2 = 0, 0.25, 0.5, 1, 2, and 3. The relative amplitudes of fluctuations considered are β = 0, 0.5, 1, and 2, while Strouhal number is kept at $\frac{\pi}{4}$, and Prandtl number at 0.71 (assuming an air flow). To facilitate comparisons during a cycle, the length of each cycle is scaled to unity by defining a dimensionless time τ, which is related to the previously defined dimensionless time t by

$$\tau = St/2\pi \tag{4}$$

The local and average Nusselt numbers (N_u, $\overline{N_u}$ are obtained from

$$N_u(\theta, \tau) = -2\left(\frac{\partial \varphi}{\partial \xi}\right)_{\xi=0} \tag{5}$$

$$\overline{N_u}(\tau) = \frac{1}{2}\int_0^\pi N_u(\theta, \tau) \sin\theta d\theta \tag{6}$$

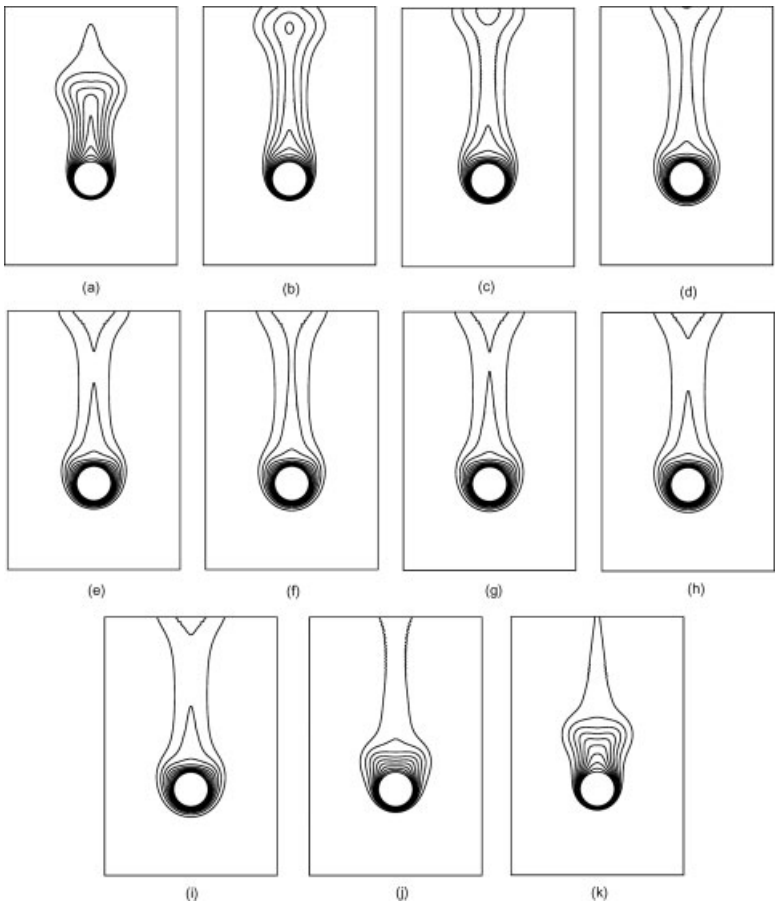

Figure 3. Isotherms for the case Re = 50, *Gr* = 2,500, and $\beta = 1$.

τ = (a) 0.0000, (b) 0.2500, (c) 0.3750, (d) 0.4900, (e) 0.5000, (f) 0.5200, (g) 0.5400, (h) 0.5600, (i) 0.5800, (j) 0.7500, (k) 0.8750. Isotherms plotted are 1, 0.9, 0.8, ...

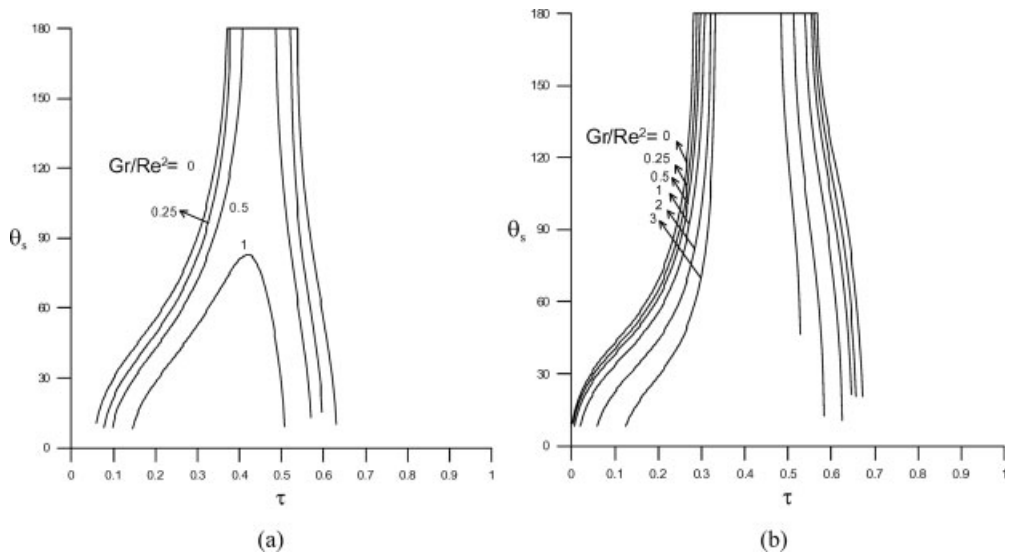

Figure 4. Variation of θ_s during one complete cycle for the case Re = 10 (a) $\beta = 1$, and (b) $\beta = 2$.

The time-averaged Nusselt number $\overline{\overline{N_u}}$ is obtained by averaging $\overline{N_u}(\tau)$ over a complete cycle and becomes constant when quasi-steady states are reached. The quantity $\overline{\overline{N_u}}$ is obtained from

$$\overline{\overline{N_u}}(\tau) = \int_{\tau-1/2}^{\tau+1/2} \overline{N_u}(x)dx \tag{7}$$

The fluid in the entire computational domain is assumed at rest at time $t = 0$ with a uniform temperature everywhere. The fluid motion starts at $t = 0$ and, at the same time, the temperature of the surface of the sphere increases from T_∞ to T_s. The computational model is then used to predict the time development of both flow and thermal fields until quasi-steady states are reached. Quasi-steady states are detected when no significant changes in the flow parameters over two complete consecutive cycles are observed. It was found that 100 cycles were quite enough to ensure such conditions. In all subsequent paragraphs, we show the results during the last cycle (that is, cycle # 100) where quasi-steady states are reached.

In general, for low-Reynolds number flows, no separation (the separation point corresponds to where surface vorticity vanishes) is observed. In fact, separation first appears at Re = 20 for the sphere case in a steady uniform free-stream. In fluctuating flows, however, and due to the adverse pressure gradients during the deceleration of the free-stream, a vortex is formed at the rear stagnation point of the sphere, which increases in size and migrates toward the front stagnation point. The depth and the breadth of the separation region are influenced by the flow velocity. The created adverse pres-

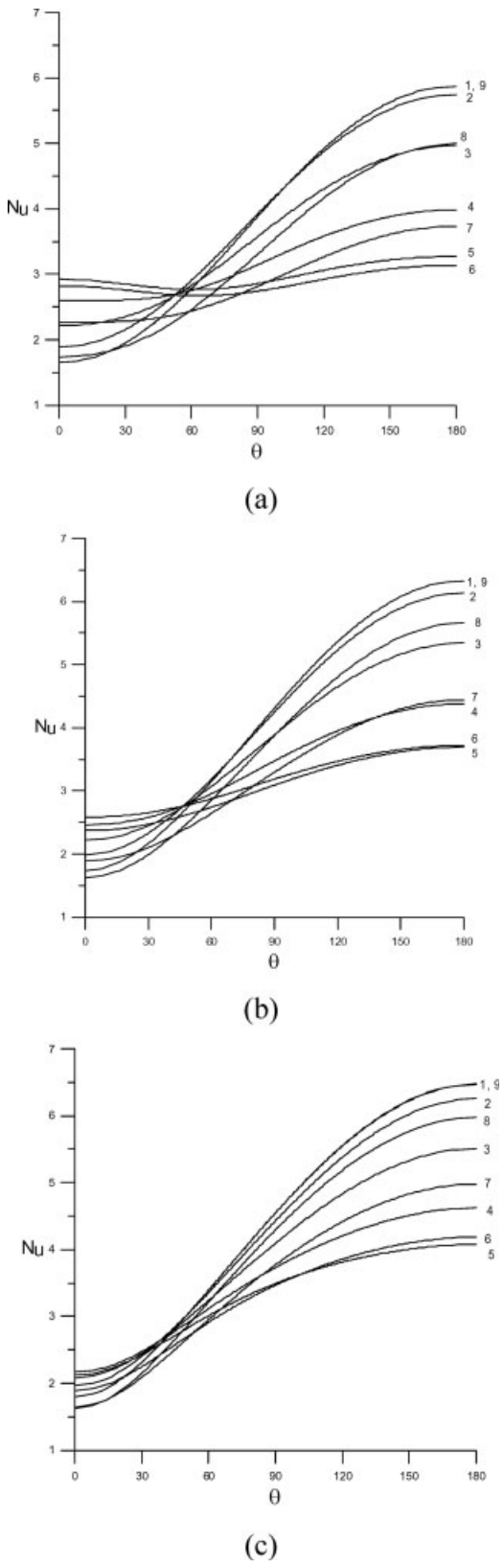

Figure 5. Variation of the local Nusselt number along the surface of the sphere during one complete cycle for the case Re = 10, $\beta = 1$, at Gr = (a) 0, (b) 100, and (c) 300.

(The times shown are: 1 ≡ 0.000, 2 ≡ 0.125, 3 ≡ 0.250, 4 ≡ 0.375, 5 ≡ 0.500, 6 ≡ 0.625, 7 ≡ 0.750, 8 ≡ 0.875, 9 ≡ 1.000).

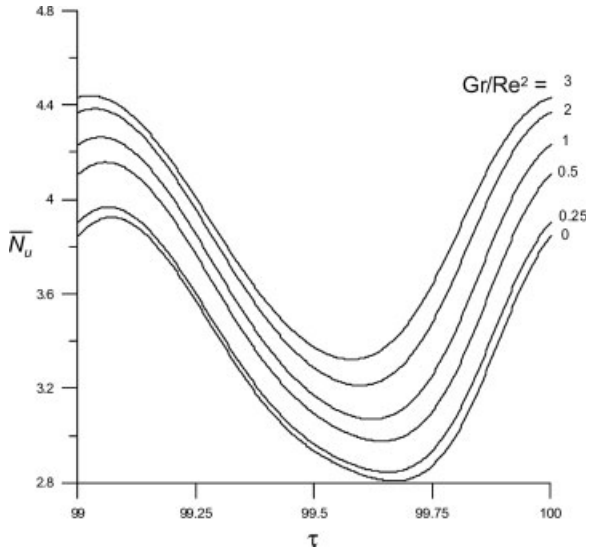

Figure 6. Variation of $\overline{N_u}$, during one complete cycle for the case Re = 10, $\beta = 1$ at different values of $\frac{Gr}{Re^2}$.

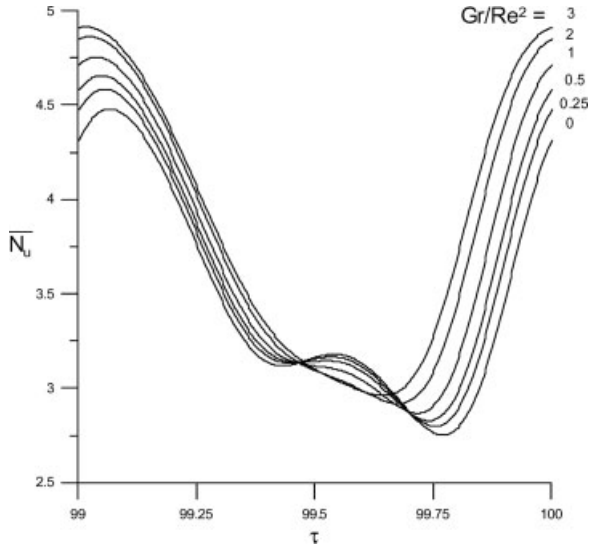

Figure 7. Variation of $\overline{N_u}$, during one complete cycle for the case Re = 10, $\beta = 2$ at different values of $\frac{Gr}{Re^2}$.

sure gradient may enlarge the formed vortex until it eventually encapsulates the whole sphere. The recirculation region withdraws back and starts to disintegrate as the free-stream starts to accelerate again. The recirculation region disappears completely until the free-stream attains enough strength to generate another region close to the start of the new cycle. The adverse pressure gradients which are held responsible for the formation of vortices are significantly altered with the introduction of the upward motion created by buoyancy forces. Increasing buoyancy forces (higher *Gr*) makes the rising convective currents strong enough to weaken and possibly destroy the vortex formation at the rear stagnation point.

We present the streamlines and isotherms for some selected case of the study. Figure 2 shows snapshots of the streamlines for the case Re = 50, Gr = 2,500 ($Gr/Re^2 = 1$), and $\beta = 1$ during one complete cycle. At the start of the cycle, and due to the relatively high-value of Re, a small vortex is already present at the wake (Figure 2a). This region may not appear for low Re values. As the free-stream decelerates, the vortex increases in size and travels toward the front stagnation point. As expected, the rising convective currents weaken the formation and shedding of the vortices at the rear stagnation point. It can be seen in Figure 2 that the formed vortex does not engulf the sphere at all. It only increases in size, but the buoyancy currents tend to retard its movement toward the front stagnation point. The corresponding isotherms are plotted in Figure 3. The contours plotted for the dimensionless temperature range from unity on the surface of the sphere to zero in the bulk fluid in intervals of 0.1. One can observe that the thermal plume, as a result of buoyancy currents, is thin and lengthened in the stream-wise direction. It should be noted that each case considered in this study produces peculiarly fascinating streamlines and isotherms.

Figure 4 confirms the dependence of the separation angle (θ_s) on Gr/Re^2 and β. The figure shows the variation of the separation angle during one complete cycle for the two cases $\beta = 1$ and $\beta = 2$, when Re = 10 at different values of Gr/Re^2. When $\beta = 1$, no separation is observed beyond $Gr/Re^2 = 1$. As mentioned earlier, the role of buoyancy forces is destructive to the formation of vortices when these forces work against the free-stream motion.

Figure 5 shows the local Nusselt number variation along the surface of the sphere for the case of Re = 10, $\beta = 1$, and at the three Grashof numbers of 0 (forced convection), 100, and 300. One can observe the significant effect of buoyancy forces on the wake region. Less variations of the local Nusselt number are observed at the back stagnation point when buoyancy forces are strong (Figure 5c). It is, therefore, of interest to find out the effect of *Gr* on the overall (average) Nusselt number, $\overline{N_u}$. Figure 6 shows the variation of $\overline{N_u}$ during one complete cycle (the last cycle) for the case of Re = 10, and $\beta = 1$ at different values of Gr/Re^2. The strength of buoyancy forces relative to inertia and viscous forces is measured through the quantity $\frac{Gr}{Re^2}$, which appears in Eq. 2.

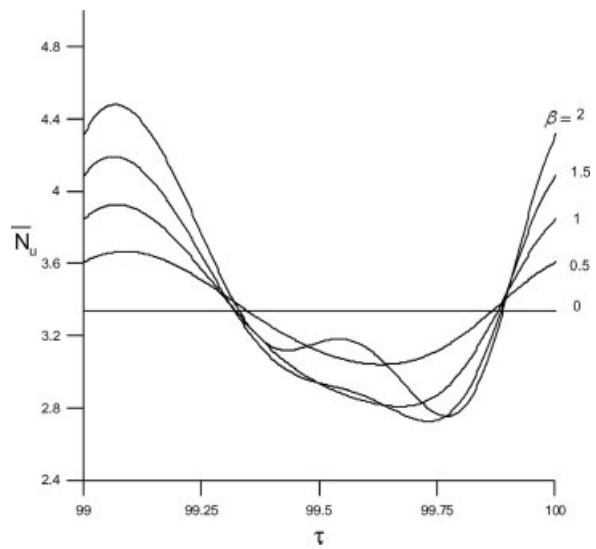

Figure 8. Variation of $\overline{N_u}$, during one complete cycle for the case Re = 10, and $Gr = 0$.

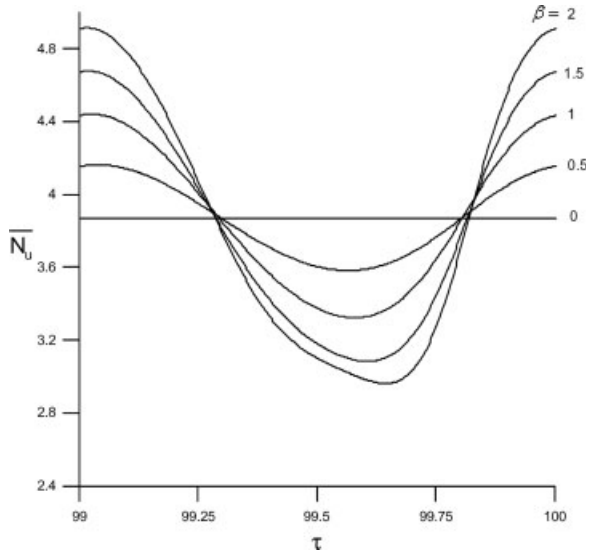

Figure 9. Variation of $\overline{N_u}$ during one complete cycle for the case Re = 10, and $Gr = 300$.

Table 1. Calculated values of $\overline{\overline{N_u}}$

	Gr/Re^2 \ β	0	0.5	1	1.5	2
Re = 10	0	3.339	3.335	3.303	3.343	3.482
	0.25	3.454	3.328	3.349	3.381	3.551
	0.5	3.540	3.394	3.516	3.430	3.600
	1	3.666	3.543	3.628	3.634	3.673
	2	3.795	3.788	3.773	3.752	3.776
	3	3.870	3.867	3.864	3.836	3.851
Re = 20	0	3.891		4.002		
	0.25	4.222		3.992		
	0.5	4.358		4.093		
	1	4.379		4.335		
	2	4.727		4.661		
	3	4.751		4.794		
Re = 50	0	5.367		5.323		
	0.25	5.748		5.578		
	0.5	6.001		5.773		
	1	6.002		6.120		
	2	6.779		7.035		
	3	7.351		7.148		
Re = 100	0	6.525		7.005		
	0.25	6.556		7.053		
	0.5	7.860		7.315		
	1	7.716		7.843		
	2	8.768		8.691		
	3	9.607		9.423		
Re = 200	0	8.670		9.559		
	0.25	9.806		9.599		
	0.5	9.104		9.974		
	1	11.335		10.557		
	2	11.869		11.508		
	3	12.514		12.395		

Figure 6 shows that $\overline{N_u}$ increases with the increase of $\frac{Gr}{\mathrm{Re}^2}$ during the whole cycle. This trend, however, is not completely true for the same case with $\beta = 2$. One can observe, Figure 7, that at some time during the cycle (nearly the middle of the cycle), $\overline{N_u}$ is higher at lower values of $\frac{Gr}{\mathrm{Re}^2}$. This is explained by the fact that during the cycle with $\beta = 1$, no reversal of the flow direction takes place. The flow, instead, decelerates to zero at mid-cycle. With $\beta = 2$, the flow reverses direction (during the period $\tau = 0.33$–0.67) and buoyancy forces, during this time, work against the flow and the transfer of heat. Consequently, a reduction in the heat-transfer coefficient is expected as the buoyancy forces increasingly retard the convection caused by the flow.

Figure 8 shows the effect of the amplitude β on the average Nusselt number. As β increases, the heat transfer increases during the time intervals, where the free-stream attains its maximum velocity, and decreases elsewhere due to the slow motion of the free-stream. Of course, one should expect a small time lag between the flow and the thermal fields. When β increases beyond the value of unity, a reversal of the flow direction takes place, and another peak in the middle of the cycle is possible (see the middle peak when $\beta = 2$ in Figure 8). This peak, however, may disappear with the increase of buoyancy forces which, during this time, retard the free-stream flow as can be seen in Figure 9.

By averaging $\overline{N_u}(\tau)$ over a complete cycle, one obtains the time-averaged Nusselt number $\overline{\overline{N_u}}$, which becomes constant when quasi-steady states are reached. Calculating $\overline{\overline{N_u}}$ provides the overall effect of the free-stream fluctuations and buoyancy forces during one complete cycle. Generally, $\overline{\overline{N_u}}$ increases with the increase of $\frac{Gr}{\mathrm{Re}^2}$ with the effect of β becoming less pronounced at high-values of $\frac{Gr}{\mathrm{Re}^2}$. Equation 2 contains both the factors $\frac{Gr}{\mathrm{Re}^2}$ and $\frac{1}{\mathrm{Re}}$. It is, therefore, expected that $\overline{\overline{N_u}}$ is influenced by both of these factors and not only $\frac{Gr}{\mathrm{Re}^2}$.

The results of this study are summarized in Table 1. The table shows the values of the space- and time-averaged Nusselt number $\overline{\overline{N_u}}$, for all the cases considered. The total number of cases is 78. All the values are calculated based on the last cycle of the simulation (that is, cycle number 100) where quasi-steady states are ensured.

Conclusion

The effects of buoyancy forces and free-stream fluctuations on mixed convection from a spherical particle are investigated in the range of Reynolds number of 10–200, Gr/Re^2 of 0–3, and for the relative amplitudes of fluctuations in the range 0–2. The study is based on the solution of the full Navier-Stokes and energy equations for an axisymmetric flow of a Boussinesq fluid.

The development of the flow and thermal fields are presented in the form of streamlines, isotherms, and local and averaged Nusselt number distributions. Several important and interesting results related to the flow and thermal fields are found.

- It was shown that separation which does not normally occur below Re = 20.4, for the sphere case, is detected well below this number due to the deceleration of the free-stream, which creates adverse pressure gradients. It was also found that increasing buoyancy forces (higher Gr) makes the rising convective currents strong enough to weaken, and possibly eliminate the formation of the vortices at the rear stagnation point.
- $\overline{N_u}$ increases with the increase of $\frac{Gr}{\mathrm{Re}^2}$ during the whole cycle of motion for $\beta < 1$. It is possible, however, that $\overline{N_u}$ becomes higher (at some time within a cycle) at lower values of $\frac{Gr}{\mathrm{Re}^2}$ for $\beta > 1$, due to the fact that the flow reverses direction and buoyancy forces, during this time, work against the flow and the transfer of heat.
- $\overline{\overline{N_u}}$ increases with the increase of $\frac{Gr}{\mathrm{Re}^2}$ with the effect of β becoming less pronounced at high-values of $\frac{Gr}{\mathrm{Re}^2}$.
- The heat-transfer rate is influenced by both Re and $\frac{Gr}{\mathrm{Re}^2}$.

Acknowledgments

We would like to express our sincere appreciation to King Fahd University of Petroleum & Minerals (KFUPM) for supporting this research under grant FT-2004/27.

Literature Cited

1. Potter JM, Riley N. Free convection from a heated sphere at large Grashof number. *J Fluid Mech*. 1980;100(4):769–783.
2. Geoola F, Cornish ARH. Numerical solution of steady-state free convective heat transfer from a solid sphere. *Int J Heat Mass Transfer*. 1981;24(8):1369–1379.
3. Geoola F, Cornish ARH. Numerical simulation of free convective heat transfer from a sphere. *Int J Heat Mass Transfer*. 1982; 25(11):1677–1687.
4. Riley N. The heat transfer from a sphere in free convective flow. *Computers & Fluids*. 1986;14(3):225–237.
5. Brown SN, Simpson CJ. Collision phenomena in free-convective flow over a sphere. *J Fluid Mech*. 1982;124:123–137.
6. Singh SN, Hasan MM. Free convection about a sphere at small Grashof number. *Int J Heat Mass Transfer*. 1983;26(5):781–783.

7. Dudek DR, Fletcher TH, Longwell JP, Sarofim AF. Natural convection induced forces on spheres at low Grashof numbers: comparison of theory with experiment. *Int. J. Heat Mass Transfer*. 1988;31(4): 863–873.
8. Dennis SCR, Walker MS. Forced convection from heated spheres. *Aeronautical Research Council*. 1964;26:105.
9. Whitaker S. Forced convection heat transfer correlations for flow in pipes, past flat plates, single cylinders, single spheres, and for flow in packed beds and tube bundles. *AIChE J*. 1972;18(21):361.
10. Dennis SCR, Walker JDA, Hudson JD. Heat transfer from a sphere at low Reynolds numbers. *J Fluid Mech*. 1973;60(2):273–283.
11. Sayegh NN, Gauvin WH. Numerical analysis of variable property heat transfer to a single sphere in high temperature surroundings. *AIChE J*. 1979;25(3):522–534.
12. Hieber CA, Gebhart B. Mixed convection from a sphere at small Reynolds and Grashof numbers. *J Fluid Mech*. 1969;38:137–159.
13. Acrivos A. On the combined effect of forced and free convection heat transfer in laminar boundary layer flows. *Chem Eng Sci*. 1966; 21:343–352.
14. Wong K-L, Lee S-C, Chen C-K. Finite element solution of laminar combined convection from a sphere. *Transactions of the ASME*. 1986;108:860–865.
15. Nguyen HD, Paik S, Chung JN. Unsteady mixed convection heat transfer from a solid sphere: the conjugate problem. *Int J Heat Mass Transfer*. 1993;36(18):4443–4453.
16. Bassett B. *A treatise in hydrodynamics*. vol. II. Deighton, Bell and Co; 1888.
17. Odar F, Hamilton S. Forces on a sphere accelerating in a viscous fluid. *J Fluid Mech*. 1964;18:302.
18. Mei R. Flow due to an oscillating sphere and an expression for unsteady drag on the sphere at finite Reynolds number. *J Fluid Mech*. 1994;270:133–174.
19. Lawrence CJ, Mei R. Long-time behavior of the drag on a body in impulsive motion. *J Fluid Mech*. 1995;283:307–327.
20. Sano T. Unsteady flow past a sphere at low Reynolds number. *J Fluid Mech*. 1981;112:433–441.
21. Lovalenti PM, Brady JF. The hydrodynamic force on a rigid particle undergoing arbitrarily time-dependent motion at small Reynolds number. *J Fluid Mech*. 1993;256:561–605.
22. Mei R, Lawrence CJ, Adrian RJ. Unsteady drag on a sphere at finite Reynolds number with small fluctuations in the free-stream velocity. *J Fluid Mech*. 1991;233:613–631.
23. Riley N. On a sphere oscillating in a viscous fluid. *Q J Mech Appl Math*. 1966;19(4).
24. Chang EJ, Maxey MR. Unsteady flow about a sphere at low to moderate Reynolds number. Part I. Oscillatory motion. *J Fluid Mech*. 1994;277:347–379.
25. Alassar RS, Badr HM. Oscillating viscous flow over a sphere. *Computers and Fluids*. 1997;26(7):661–682.
26. Drummond CK, Lyman FA. Mass transfer from a sphere in an oscillating flow with zero mean velocity. *Comput Mech*. 1990;6:315–326.
27. Ha MY, Yavuzkurt S. A theoretical investigation of acoustic enhancement of heat and mass transfer I. Pure oscillating flow. *Int J Heat Mass Transfer*. 1993;36(8):2183–2192.
28. Ha MY, Yavuzkurt S. A theoretical investigation of acoustic enhancement of heat and mass transfer II. Oscillating flow with a steady velocity component. *Int J Heat Mass Transfer*. 1993; 36(8):2193–2202.
29. Alassar RS, Badr HM, Mavromatis HA. Heat convection from a sphere placed in an oscillating free stream. *Int J Heat Mass Transfer*. 1999;42:1289–1304.

Manuscript received July 18, 2006, and revision received Mar. 13, 2007.